Electronic Supplementary Information (ESI)

Controlled *In Situ* Reaction in Assembly of Cu(II) Mixed-ligand Coordination Polymers: Synthesis, Structure, *In-situ* Reaction

Xing-Po Wang,[a] Ya-Qin Zhao,[a] Zvonko Jagličić,[b] Su-Na Wang,[c] Shu-Jie Lin,[a] Xiao-Yi Li,[a] Di Sun*,[a]

[a]Key Lab of Colloid and Interface Chemistry, Ministry of Education, School of Chemistry and Chemical Engineering, Shandong University, Jinan, 250100, P. R. China.

Email: dsun@sdu.edu.cn

[b]Faculty of Civil and Geodetic Engineering & Institute of Mathematics, Physics and Mechanics, University of Ljubljana, Jamova 2, 1000 Ljubljana, Slovenia.

[c]School of Chemistry and Chemical Engineering, Liaocheng University, Liaocheng, People's Republic of China.

1. Table S1. Selected bond lengths and angles for 1.

CU1—N3	1.979 (5)	CU3—N6^{III}	1.982 (6)
Cu1—N4	1.978 (6)	Cu3—O2^{iv}	2.333 (5)
Cu1—O1	1.968 (5)	Cu3—O7	1.944 (5)
Cu1—O1W	2.345 (5)	Cu3—O8	1.886 (6)
Cu1—O3	1.939 (4)	Cu4—N2^{ii}	1.999 (6)
Cu2—N5	1.980 (6)	Cu4—O2W	2.402 (11)
Cu2—O3	1.917 (5)	Cu4—O4^{v}	2.675 (5)
Cu2—O4	1.928 (5)	Cu4—O5^{v}	2.010 (5)
Cu2—O6	1.980 (5)	Cu4—O8	1.932 (6)
Cu2—O10^{i}	2.375 (5)	Cu4—O9	1.947 (5)
Cu3—N1^{ii}	1.968 (5)		
N3—Cu1—O1W	89.0 (2)	O7—Cu3—N1^{ii}	172.8 (2)
N4—Cu1—N3	96.8 (2)	O7—Cu3—N6^{iii}	90.1 (2)
N4—Cu1—O1W	97.0 (2)	O7—Cu3—O2^{iv}	92.7 (2)
O1—Cu1—N3	91.4 (2)	O8—Cu3—N1^{ii}	87.3 (2)
O1—Cu1—N4	169.0 (2)	O8—Cu3—N6^{iii}	154.3 (3)
O1—Cu1—O1W	90.5 (2)	O8—Cu3—O2^{iv}	103.6 (2)
O3—Cu1—N3	165.9 (2)	O8—Cu3—O7	85.9 (2)
O3—Cu1—N4	87.1 (2)	N2^{ii}—Cu4—O2W	92.1 (3)
O3—Cu1—O1	83.22 (19)	N2^{ii}—Cu4—O4^{v}	92.0 (2)
O3—Cu1—O1W	104.0 (2)	N2^{ii}—Cu4—O5^{v}	92.5 (2)
N5—Cu2—O10^{i}	91.8 (2)	O2W—Cu4—O4^{v}	140.9 (3)
O3—Cu2—N5	85.0 (2)	O5^{v}—Cu4—O2W	86.9 (3)
O3—Cu2—O4	93.55 (19)	O5^{v}—Cu4—O4^{v}	54.10 (17)
O3—Cu2—O6	170.7 (2)	O8—Cu4—N2^{ii}	86.9 (2)
O3—Cu2—O10^{i}	92.5 (2)	O8—Cu4—O2W	104.9 (3)
O4—Cu2—N5	178.3 (2)	O8—Cu4—O4^{v}	114.1 (2)
O4—Cu2—O6	92.2 (2)	O8—Cu4—O5^{v}	168.2 (3)
O4—Cu2—O10^{i}	89.1 (2)	O8—Cu4—O9	91.3 (2)
O6—Cu2—N5	89.2 (2)	O9—Cu4—N2^{ii}	177.5 (2)
O6—Cu2—O10^{i}	94.95 (19)	O9—Cu4—O2W	86.8 (3)
N1^{ii}—Cu3—N6^{iii}	95.2 (2)	O9—Cu4—O4^{v}	90.2 (2)
N1^{ii}—Cu3—O2^{iv}	91.0 (2)	O9—Cu4—O5^{v}	89.6 (2)
N6^{iii}—Cu3—O2^{iv}	102.0 (2)		
Symmetry codes: (i) −*x*, −*y*+1, −*z*; (ii) *x*+1, −*y*+3/2, *z*−1/2; (iii) *x*+1, *y*, *z*; (iv) *x*, −*y*+3/2, *z*−1/2; (v) −*x*+1, −*y*+1, −*z*.			

2. Figure S1. UV-Vis spectrum of 1.

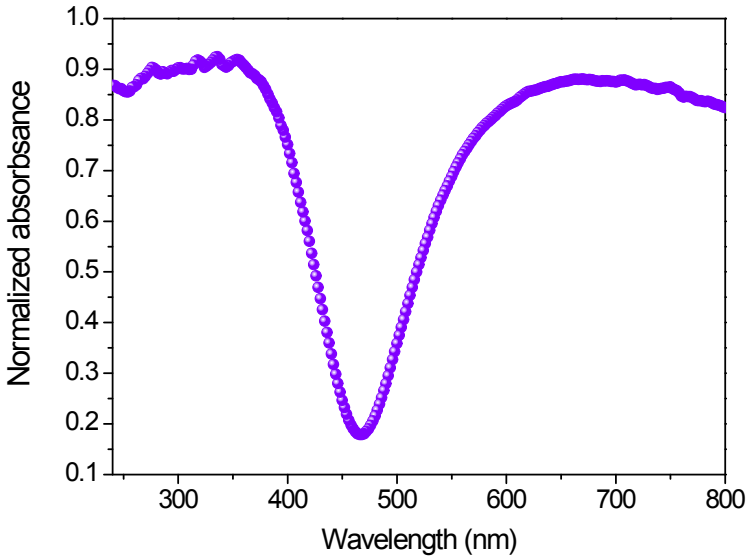

3. Figure S2. The XRD patterns of 1.

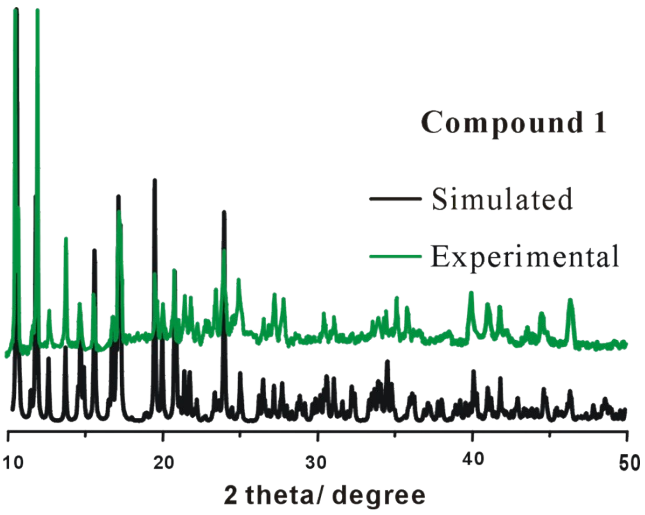

As shown in Fig. S2, the X-ray powder diffraction patterns measured for the as-synthesized sample of **1** is in good agreement with the PXRD patterns simulated from the respective single-crystal X-ray data, proving the purity of the bulk phases. The dissimilarity in reflection intensities between the simulated and the experimental patterns may be due to the different orientation of the microcrystals in the powder samples.

4. Figure S3. The TGA for 1.

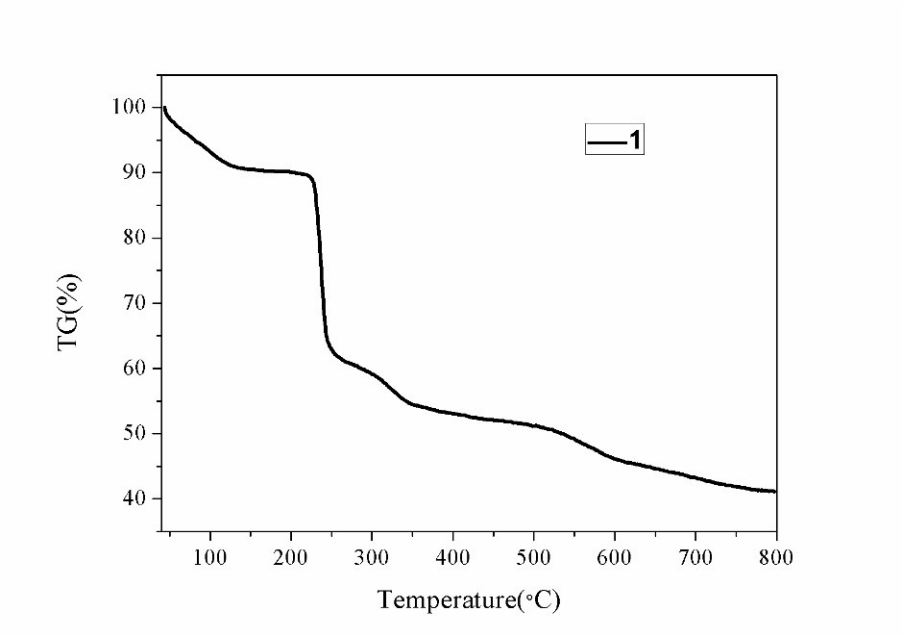

5. Figure S4. The IR for 1.

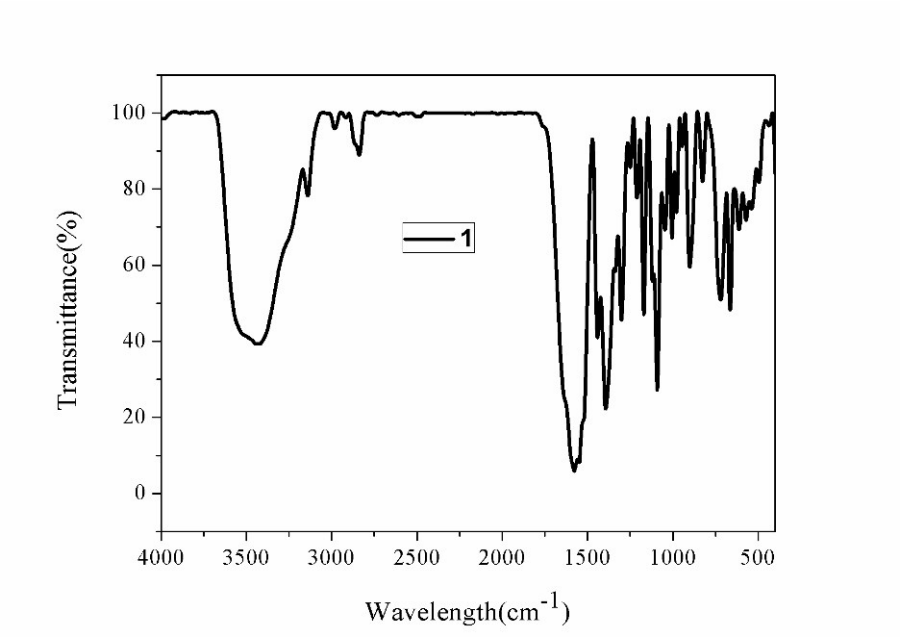

6. Figure S5-S10 ^{1}H NMR spectra for reaction mixtures after catalysis by 1.

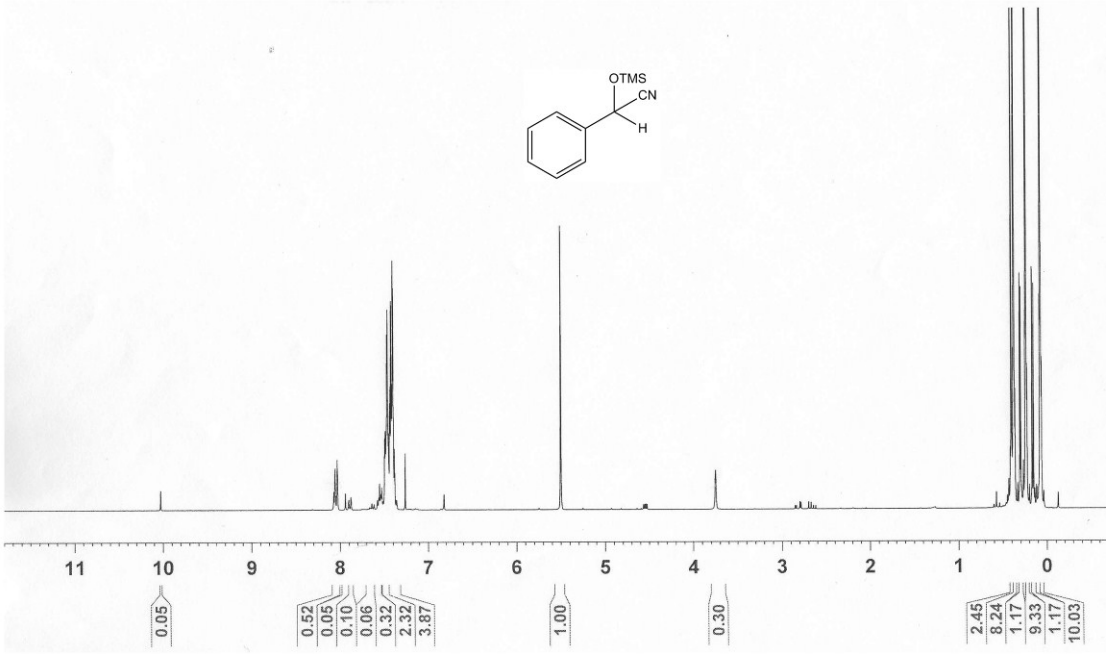

(a) ^{1}H NMR of crude reaction mixture corresponding to Table1, entry 1.

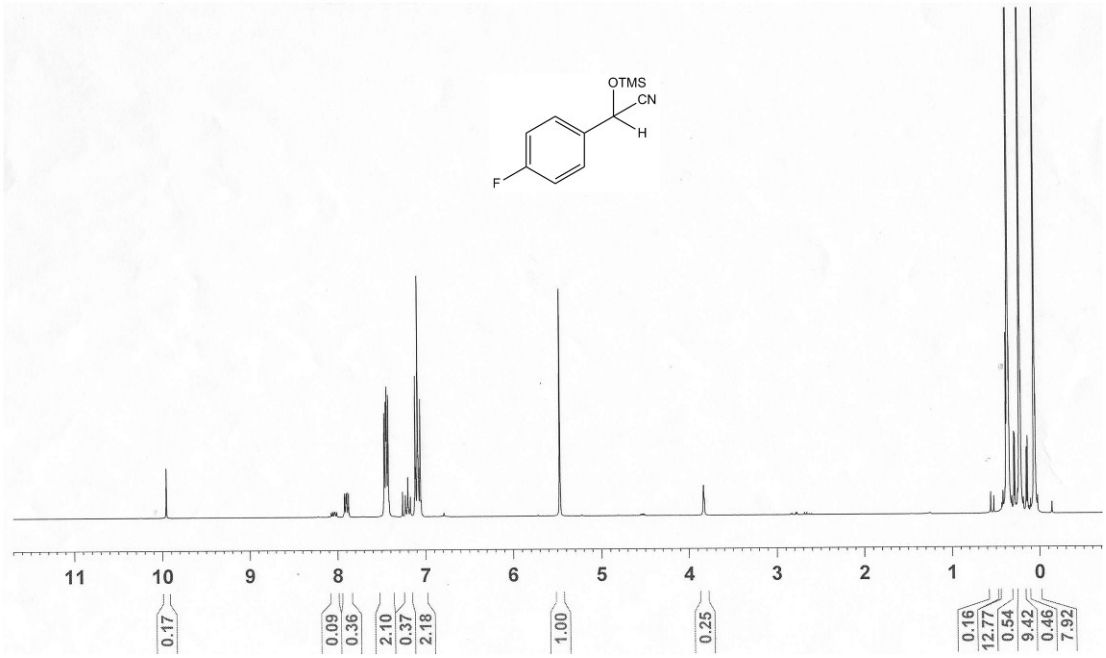

(b) ^{1}H NMR of crude reaction mixture corresponding to Table1, entry 2.

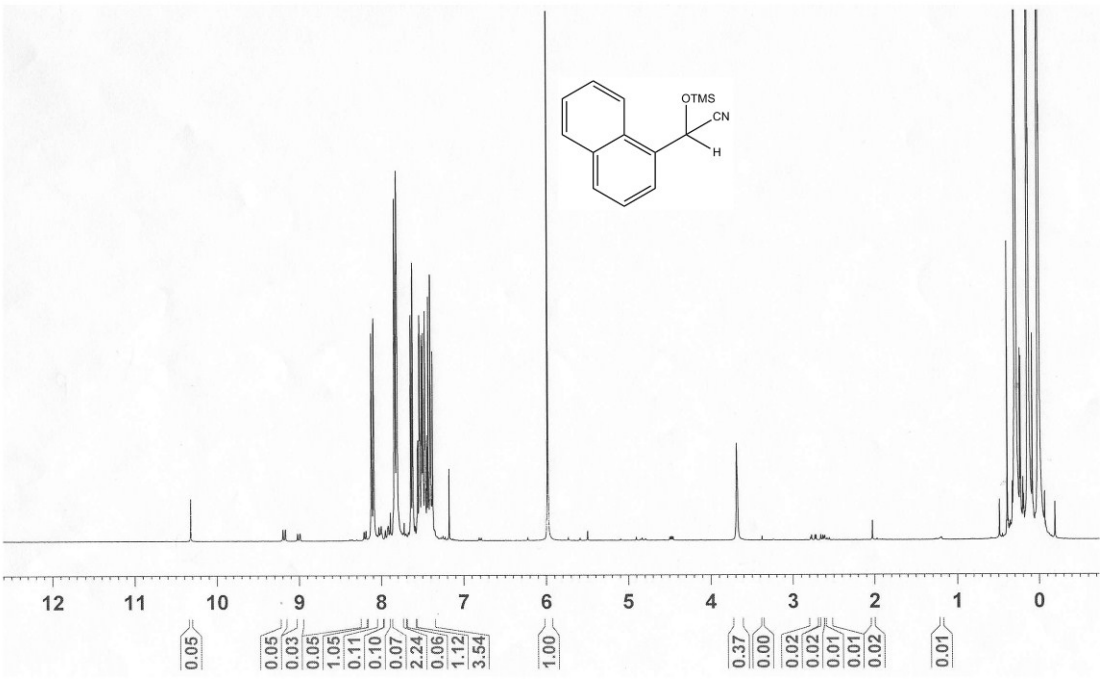

(c) ^{1}H NMR of crude reaction mixture corresponding to Table1, entry 3.

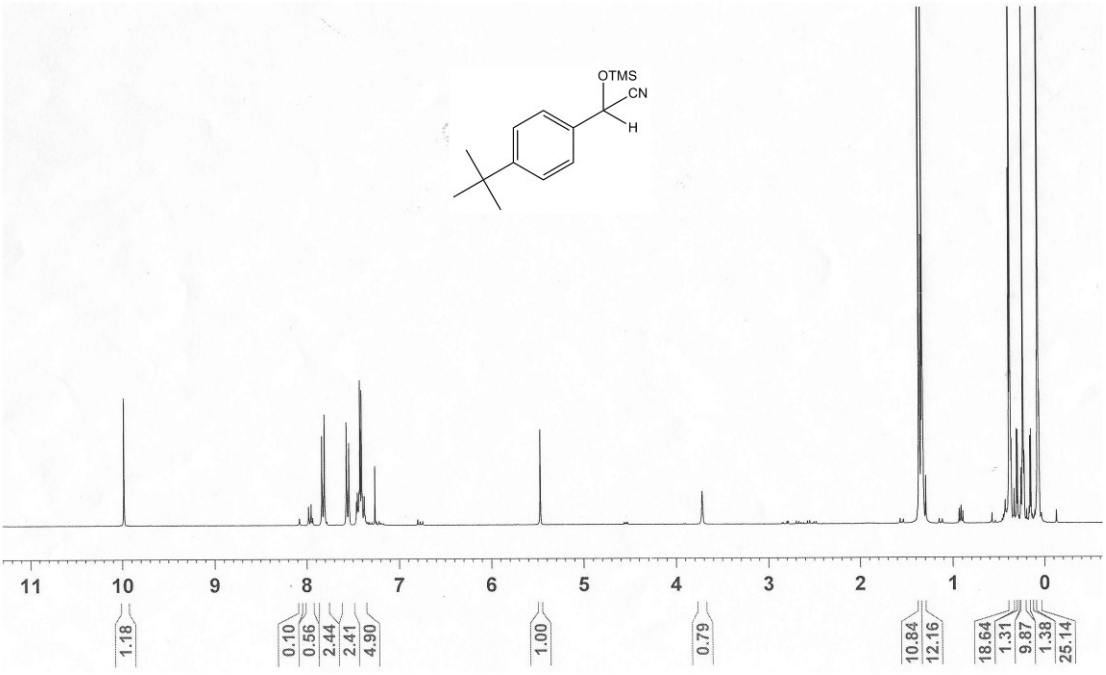

(d) ^{1}H NMR of crude reaction mixture corresponding to Table1, entry 4.

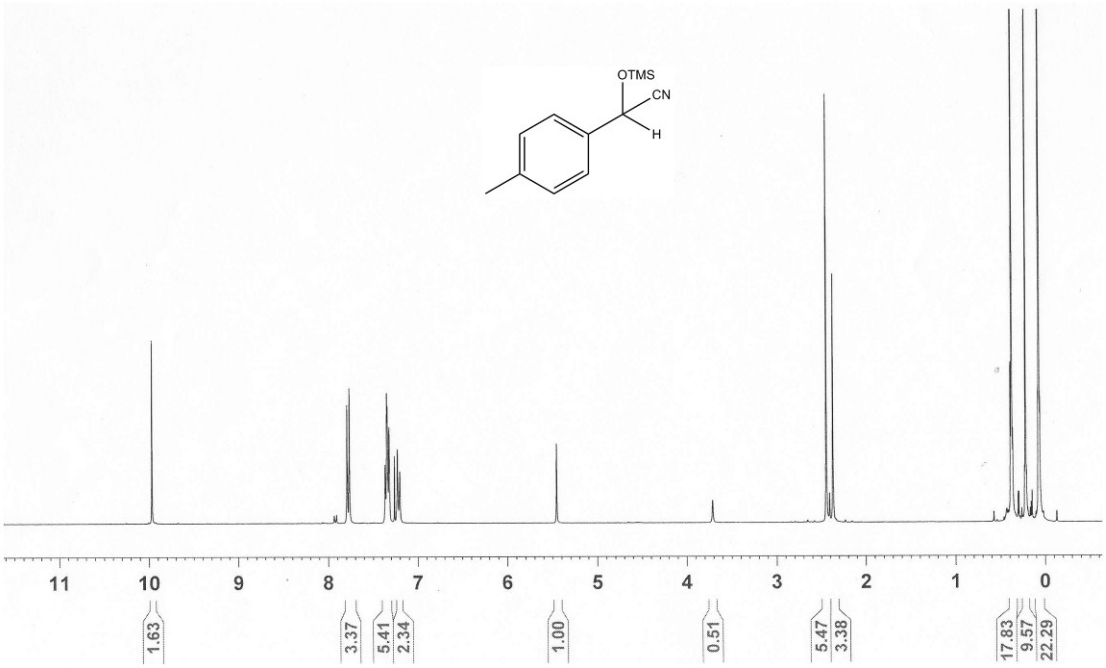

(e) ^{1}H NMR of crude reaction mixture corresponding to Table1, entry 5.

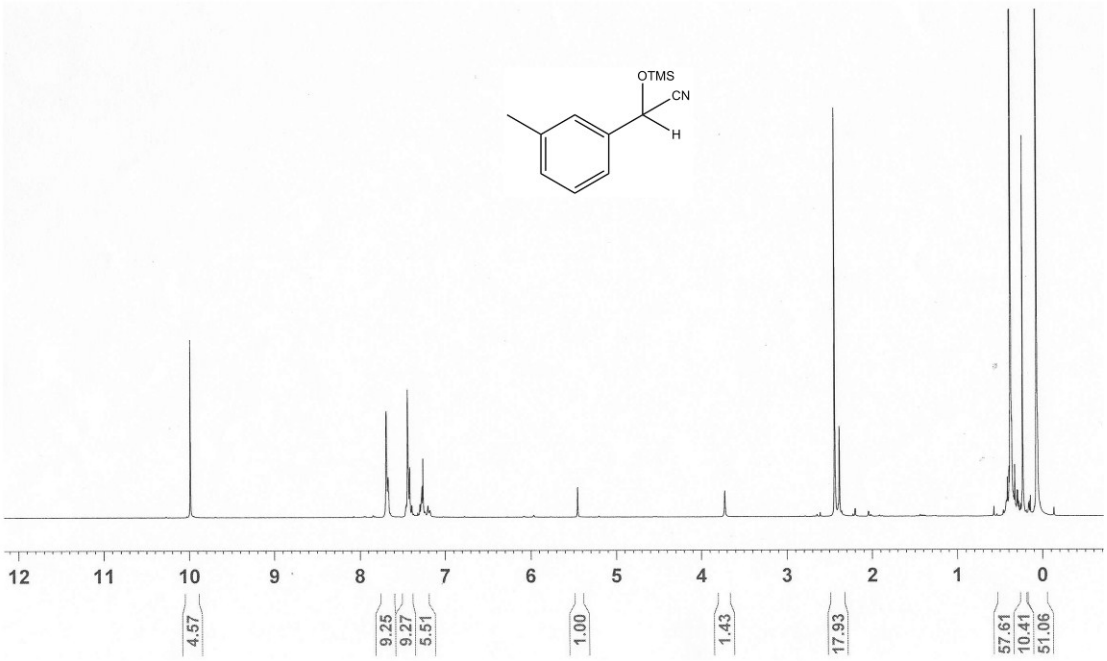

(f) ^{1}H NMR of crude reaction mixture corresponding to Table1, entry 6.

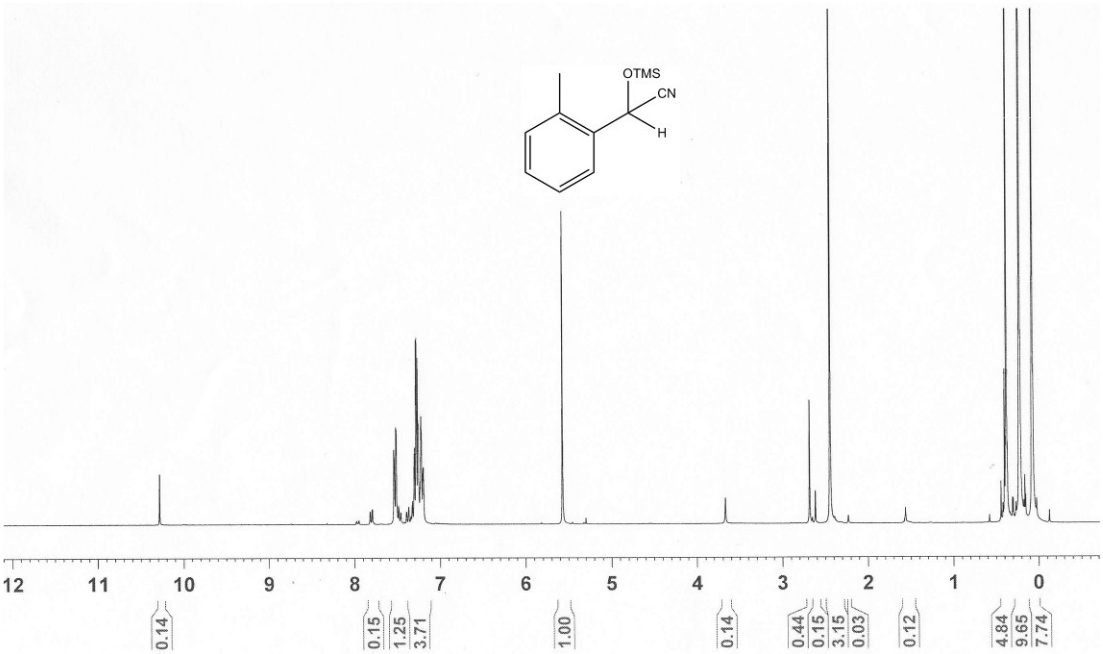

(g) ^{1}H NMR of crude reaction mixture corresponding to Table1, entry 7.

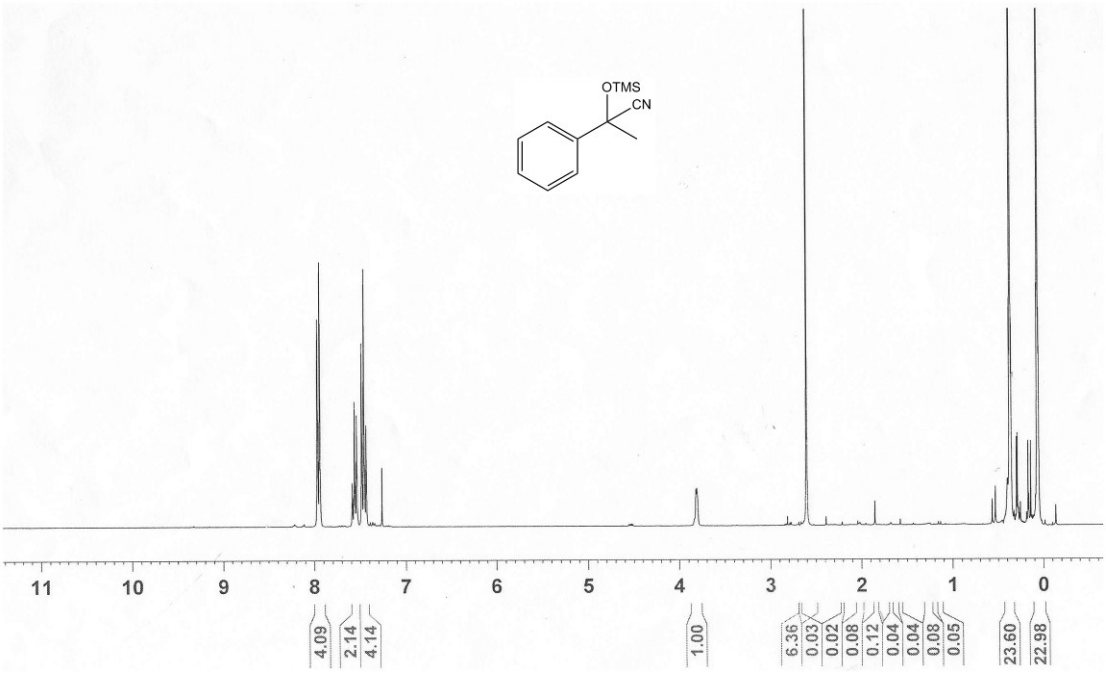

(h) ^{1}H NMR of crude reaction mixture corresponding to Table1, entry 8.

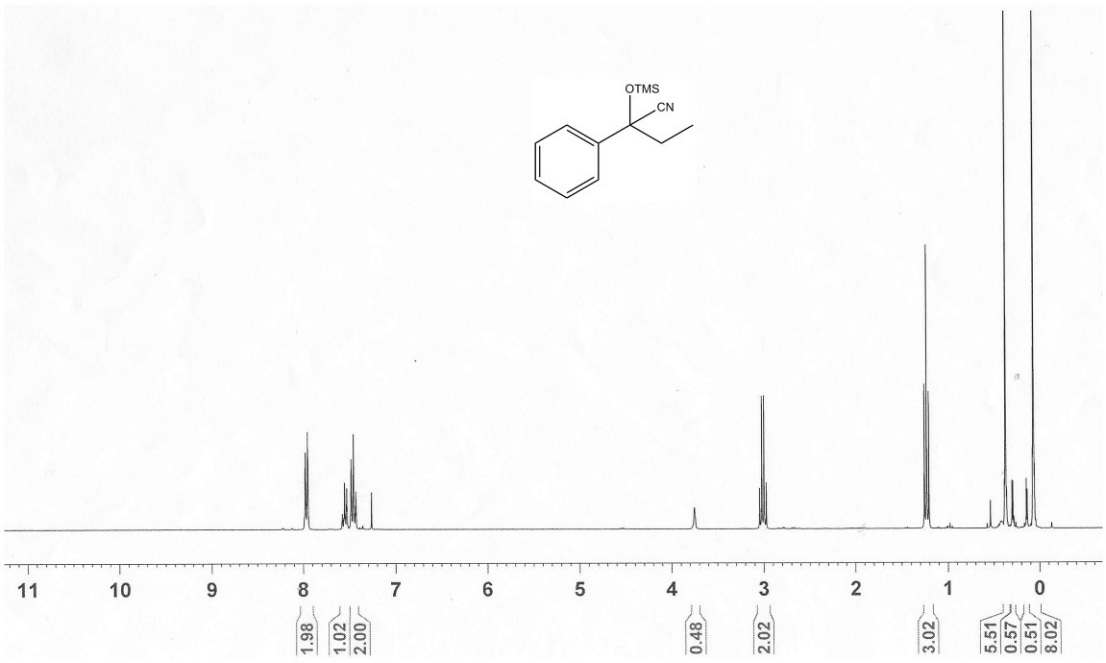

(i) ^{1}H NMR of crude reaction mixture corresponding to Table1, entry 9.

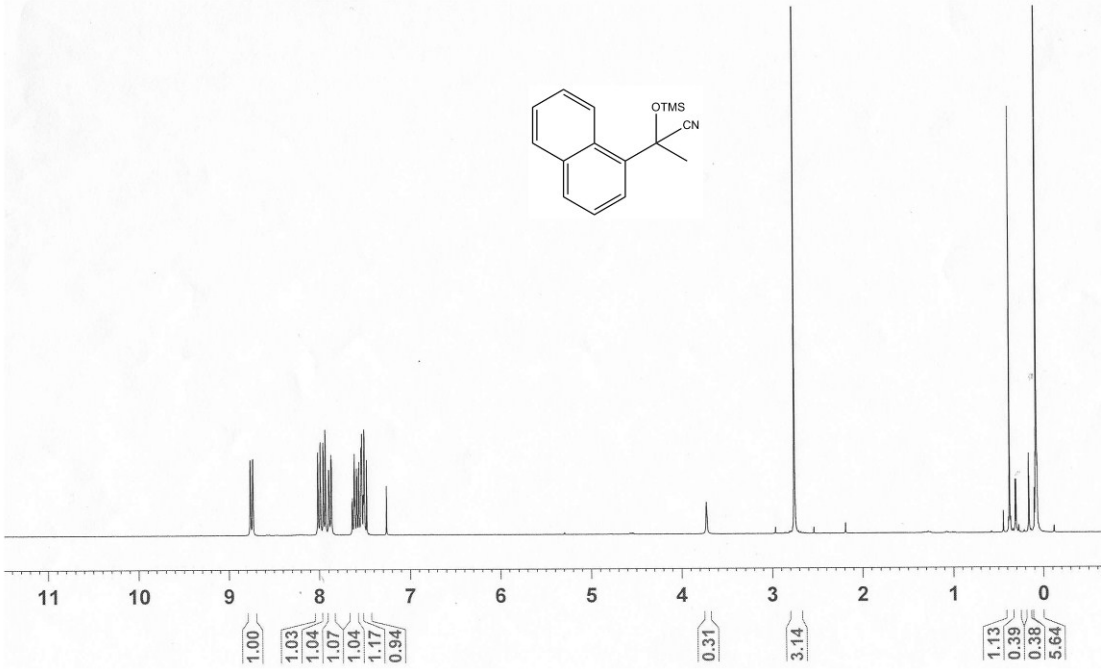

(j) ^{1}H NMR of crude reaction mixture corresponding to Table1, entry 10.